Photoinduced Hubbard band mixing due to ultrafast laser irradiation of a one-dimensional Mott insulator

J. D. Lee[1] and J. Inoue[2]
[1]*School of Materials Science, Japan Advanced Institute of Science and Technology, Ishikawa 923-1292, Japan*
[2]*Quantum Dot Research Center, National Institute for Materials Science, Tsukuba 305-0044, Japan*
(Received 10 August 2007; published 28 November 2007)

Based on the nonperturbative many-body time-dependent approach, photoinduced Hubbard band mixing by ultrashort laser pulse is found in a one-dimensional half-filled Hubbard model through the optical conductivity. The nonlinear development of Drude-like (metallic) weight in the resonant optical pumping ($\omega_{\mathrm{pu}} \approx E_g$; ω_{pu} is the pumping laser energy and E_g is the gap energy) indicates reconstruction and mixing of the upper and lower Hubbard bands, in contrast to the case of linear development in off-resonant pumping ($\omega_{\mathrm{pu}} \gg E_g$) where the rigid band picture is valid. The photoemission response after the ultrashort pulse confirms our finding.

DOI: 10.1103/PhysRevB.76.205121 PACS number(s): 78.20.Bh, 78.47.+p, 78.67.−n, 79.60.−i

Photoinduced phase transitions (PIPTs) in correlated systems attract increasing attention and provide a benchmarking cornerstone for a new field of photodynamics. This recent focus is due not only to basic scientific interest but also to PIPTs' implicit potential for device applications, such as ultrafast switches.[1] A rather wide range of materials shows such PIPTs by an intrinsic instability due to a cooperative interaction among electronic, magnetic, and structural degrees of freedom.[2,3] Among these, one noticeable PIPT is the photoinduced insulator-metal transition (PIIMT) without structural changes.[4] It has been a central research subject in condensed matter physics to investigate the insulator-metal transition (IMT) of the strongly correlated electron system (SCES), which is externally controlled by chemical doping.[5]

Ultrashort optical pumping is also a useful doping method as good as chemical doping. Indeed, the onset of Drude-like weights just after the photoirradiation, which is a characteristic of PIIMT, has been reported in SCES without structural changes; the one-dimensional (1D) halogen-bridged Ni-chain compound (Ni-X chain) $[\mathrm{Ni(chxn)_2Br}]\mathrm{Br_2}$ (chxn =cyclohexanediamine).[4] There is, however, a fundamental difference between chemical and photo (optical) doping: the former is static and the latter is a dynamic phenomenon. The explicit dynamical response of SCES during the relevant ultrafast time span after ultrashort optical pumping is an unexplored problem, partially because of a lack of a theoretical framework to tackle the problem. Maeshima and Yonemitsu have tried to study theoretically the optical conductivity of the photoexcited half-filled 1D Hubbard model, where the Kubo formula was employed not for the ground state but for the first photoexcited state.[6] In such a conventional theoretical treatment, the Hubbard bands are considered to be rigid. However, it is not clear at all whether the rigid band picture can be really justified or not. This problem is a highly nontrivial and rather fundamental issue for a wide range of material science research fields.

For a theoretical study of ultrafast dynamics, a new nonperturbative formalism called many-body time-dependent diagonalization (MTD) is found to be powerful. This consists of solving the time-dependent Schrödinger equation within the many-body Hilbert space.[7,8] MTD is, in fact, good at describing the two-body responses with nonequilibrium states, which naturally reduces to the Kubo formula in the limit of a continuous optical wave in its linear order.[8,9]

In this paper, we explore electronic reconstruction in SCES by studying the optical conductivity of the half-filled 1D Hubbard system induced by ultrashort optical pumping within MTD. For this purpose, we first examine how the metallic states evolve. The photoinduced weights appear below the gap and are found to be Drude-like metallic ones. In particular, the qualitative behavior of these weights is found to depend strongly on whether the optical pumping (with laser energy ω_{pu}) is resonant ($\omega_{\mathrm{pu}} \approx E_g$) or off resonant ($\omega_{\mathrm{pu}} \gg E_g$) with the gap energy E_g. Finally, the Hubbard band reconstruction is clearly visualized through examining the photoemission response just after the ultrashort irradiation, i.e., the illuminated photoemission spectroscopy (ILPES). ILPES is also treated within MTD.

We start with the half-filled 1D Hubbard model $\mathcal{H}_0$. It is combined with the ultrashort optical pumping $\mathcal{V}$ with the polarization along the chain direction and extended to be $\mathcal{H}=\mathcal{H}_0+\mathcal{V}(\tau)$:

$$\mathcal{H}_0 = -t\sum_{l\sigma}(c^{\dagger}_{l+1\sigma}c_{l\sigma} + c^{\dagger}_{l\sigma}c_{l+1\sigma}) + U\sum_{l} n_{l\uparrow}n_{l\downarrow},$$

$$\mathcal{V}(\tau) = \hat{j}A_{\mathrm{pu}}e^{i\omega_{\mathrm{pu}}\tau}\Theta'(\tau) + \mathrm{H.c.}, \tag{1}$$

where $c^{\dagger}_{l\sigma}$ ($c_{l\sigma}$) is the electron creation (annihilation) operator with spin σ at site l and $n_{l\sigma}=c^{\dagger}_{l\sigma}c_{l\sigma}$. When this model is applied to a 1D Ni-X chain, $c^{\dagger}_{l\sigma}$ ($c_{l\sigma}$) signifies a $3d$ outer-shell electron of Ni ($\mathrm{Ni^{3+}}$). The parameter t gives the nearest-neighbor hopping and U the on-site repulsion. $\hat{j}$ is the current operator defined by $\hat{j}=it\Sigma_{l\sigma}(c^{\dagger}_{l+1\sigma}c_{l\sigma}-c^{\dagger}_{l\sigma}c_{l+1\sigma})$. For parameters of the pumping laser pulse, A_{pu} is the electric field strength and $\Theta'(\tau)=\Theta(\tau)-\Theta(\tau-\Delta)$ with the pulse length Δ [$\Theta(\tau)$ is the Heaviside step function]. For an implementation of MTD, one first needs to set up the many-body Hilbert space spanned by states of $\Pi_l|\psi^i_l\rangle$, where $|\psi^i_l\rangle$ should be the electronic state at site l, that is, $|0\rangle$, $|\uparrow\rangle$, $|\downarrow\rangle$, $|\uparrow\downarrow\rangle$ according to $i=0,1,2,3$, respectively. Within the Hilbert space, one can write down the quantum state of the whole system at time τ as $|\Psi(\tau)\rangle=\Sigma_{\{i\}}C_{\{i\}}(\tau)\Pi_l|\psi^i_l\rangle$. By exact diagonalization, one

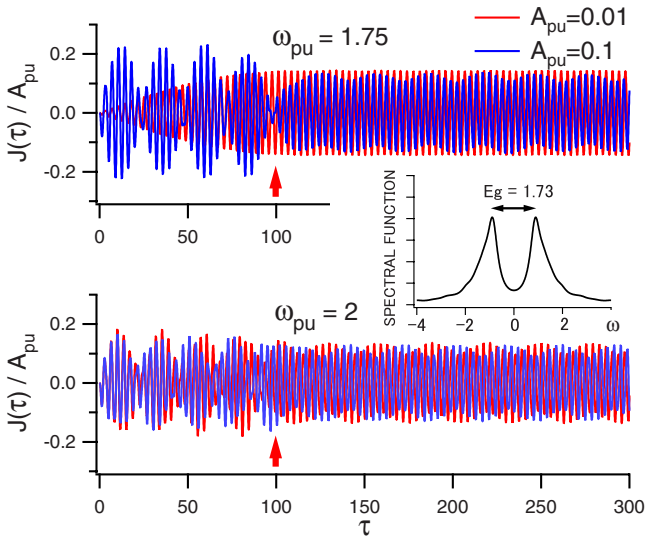

FIG. 1. (Color online) Time-dependent current $J(\tau)$ divided by the pumping electric field strength A_{pu}. $U=3$ and $t=1$ are taken for intrinsic parameters of the Hubbard model and $\Delta=100$ for the ultrashort laser pulse. The inset gives the spectral function of the system. The red arrows indicate termination of the optical pumping.

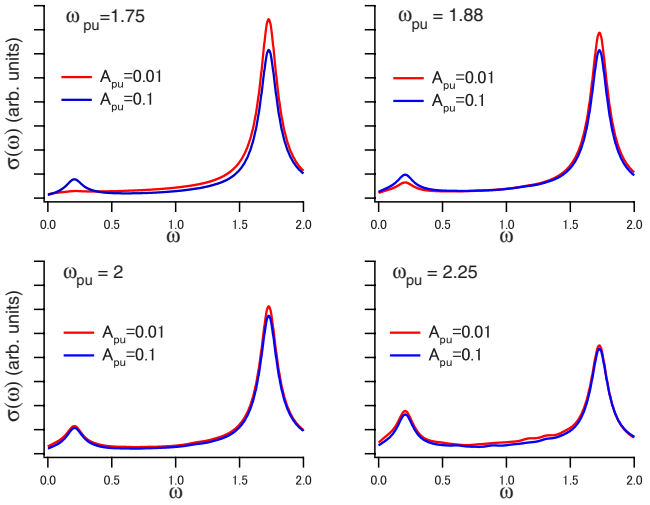

FIG. 2. (Color online) Optical conductivity $\sigma(\omega)$ from Eq. (3) with respect to ω_{pu} and A_{pu}. $U=3$ and $t=1$ are taken for intrinsic parameters of the Hubbard model.

can obtain the ground state for $|\Psi(0)\rangle$ for the half-filled 1D Hubbard model with a finite number of sites. Dynamics that starts by turning on the optical pumping at $\tau=0$ can then be described by solving the coupled differential equations for $C_{\{i\}}(\tau)$ resulting from the time-dependent Schrödinger equation $i\partial/\partial\tau|\Psi(\tau)\rangle=\mathcal{H}|\Psi(\tau)\rangle$. This is the basic scheme of MTD. From the solution, one can calculate the time-dependent optical current

$$J(\tau)=\langle\Psi(\tau)|\hat{j}|\Psi(\tau)\rangle. \tag{2}$$

$J(\tau)$ can be shown to give the usual correlation function (that is, the Kubo formula) under the linear response by the S-matrix expansion.[8,9] We treat the half-filled $N=8$ Hubbard chain with a periodic boundary condition imposed.[10] According to the symmetry arguments of the electron number and the total spin (total spin $S=0$), the effective number of bases is 4900.

In Fig. 1, the time-dependent optical current $J(\tau)$ divided by the field strength A_{pu} is provided with respect to ω_{pu} and A_{pu}. We consider the Hubbard model with $U=3$ and $t=1$ and the ultrashort pulse with $\Delta=100$. To be explicit, for $t=1$ eV, we have $\Delta=100$ eV$^{-1}\approx 66$ fs. The spectral function given in the inset of Fig. 1 shows the gap energy $E_g\approx 1.73$. In Fig. 1, it is found that $J(\tau)$ oscillates in a complicated way depending on ω_{pu} and A_{pu} when $\tau<\Delta$, but in a simple way, with a rapid oscillation sitting on a slow oscillation, when $\tau>\Delta$. The dynamics can be seen more clearly from the optical conductivity $\sigma(\omega)$ in the frequency domain. This can be obtained by the Fourier transformation of $J(\tau)/A_{\mathrm{pu}}$. For the time integral necessary for the Fourier transformation, one needs to consider practically the finite upper bound τ_c instead of $+\infty$,

$$\sigma(\omega)=\int_{\Delta}^{\tau_c} d\tau e^{i\omega\tau}[J(\tau)/A_{\mathrm{pu}}]. \tag{3}$$

In Fig. 2, $\sigma(\omega)$ is given with respect to ω_{pu} and A_{pu}. We have taken $\tau_c=1000$. From Fig. 2, it is seen that the optical conductivity consists of two peaks. One is the strong peak at the position of E_g (≈ 1.73) and the other is the low energy peak at $\omega\approx 0.22$. From $J(\tau)/A_{\mathrm{pu}}$ in Fig. 1, it can be seen that a rapid oscillation after $\tau=\Delta$ corresponds to the strong peak at the gap transition and a slow oscillation to the low energy feature, respectively. As ω_{pu} increases, a continuous transfer of the optical weight from the gap transition to the inside of the gap region is found. Interestingly, the low energy features are shown to develop nonlinearly with the external optical pumping for $\omega_{\mathrm{pu}}\approx E_g$ while developing linearly for $\omega_{\mathrm{pu}}\gg E_g$.

It is essential to understand the origin of the low energy features. In Fig. 3(a), the list of 4900 eigenvalues is illustrated. The listed eigenvalues represent corresponding eigenstates with zero double occupancy (DO), 1DO, 2DO, 3DO, and 4DO. Excitation by optical pumping from the antiferromagnetic ground state incorporates mixing of the eigenstates and leads to the optically excited state $|\Psi(\Delta)\rangle$ at $\tau=\Delta$. When $\tau>\Delta$, $J(\tau)$ can be expressed as $J(\tau)=\langle\Psi(\Delta)|e^{-i\mathcal{H}_0\tau}\hat{j}e^{i\mathcal{H}_0\tau}|\Psi(\Delta)\rangle$. Inserting a set of eigenstates $|n\rangle$ ($|n'\rangle$), i.e., $n,n'=0,\ldots,4899$ with corresponding eigenenergies $E_n(E_{n'})$, we have $J(\tau)$ in a figurative form as follows:

$$J(\tau)=\sum_n\sum_{n'}\langle\Psi(\Delta)|n'\rangle\langle n|\Psi(\Delta)\rangle\langle n'|\hat{j}|n\rangle e^{-i(E_{n'}-E_n)\tau}.$$

The following three cases can be considered to understand contributions to $J(\tau)$. First, if $n,n'\in$ 0DO, we readily find $\langle n'|\hat{j}|n\rangle=0$. This means no contribution to $J(\tau)$ from $n,n'\in$ 0DO. Second, if $n\in$ 0DO and $n'\in$ 1DO, as is evident in Fig. 3(a′), we have the strong gap transition at $E_{n'}-E_n\approx E_g$ but

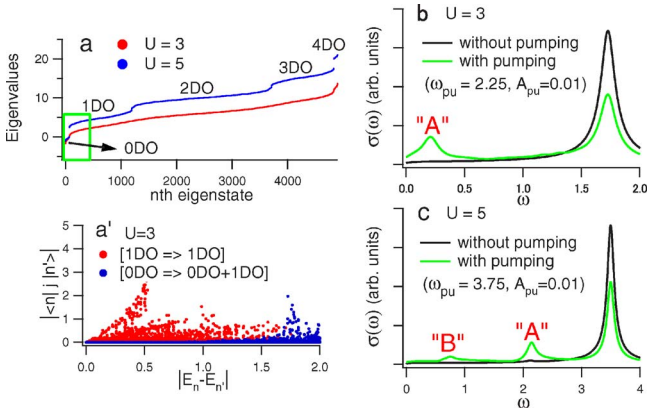

FIG. 3. (Color online) (a) List of 4900 eigenvalues for $U=3$ and $U=5$. Listed eigenvalues represent corresponding eigenstates with 0DO, 1DO, 2DO, 3DO, and 4DO. (a′) With states belonging to the green rectangle in (a) (for $U=3$), the matrix elements for $\hat{j}$ are given. [(b) and (c)] Typical comparison of optical conductivity with and without optical pumping for $U=3$ ($E_g \approx 1.73$) and $U=5$ ($E_g \approx 3.5$). "A" indicates the metallic transition within the 1DO subspace and "B" within the 2DO subspace. $t=1$ is fixed.

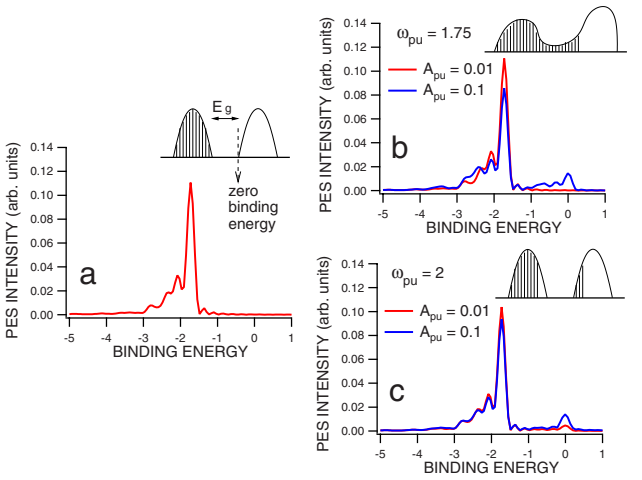

FIG. 4. (Color online) Photoemission spectra and schematic sketches of the underlying electronic structure. (a) Photoemission without optical pumping, (b) illuminated photoemission under resonant optical pumping, i.e., $\omega_{\mathrm{pu}} \approx E_g$, and (c) illuminated photoemission under off-resonant optical pumping, i.e., $\omega_{\mathrm{pu}} \gg E_g$. $U=3$ and $t=1$ are taken for intrinsic Hubbard parameters ($E_g \approx 1.73$).

little contribution from the low energy transition. Third, we consider the case of $n, n' \in$ 1DO. It is important to note that, according to Fig. 3(a′), low energy optical transitions responsible for the feature "A" [see Fig. 3(b) for $U=3$] are dominated by transitions within the 1DO subspace, which is consistent with the metallic transition by photoexcited carriers. However, we have no true Drude feature at exactly $\omega=0$ in a finite system because of $\langle n'|\hat{j}|n\rangle \to 0$ for $E_{n'}-E_n=0$. Instead, the Drude-like metallic feature will be shifted to a small nonzero value of ω,[11] that is, "A" for $U=3$ in Fig. 3(b) and "A" and "B" for $U=5$ in Fig. 3(c).

Now, we return to Fig. 2 and examine the deeper nature of IMT incorporating the development of low energy metallic features in $\sigma(\omega)$ with respect to ω_{pu} and A_{pu}. In the figure, one finds that the metallic weight develops linearly at off-resonant pumping with $\omega_{\mathrm{pu}} \gg E_g$, but it develops nonlinearly at resonant pumping with $\omega_{\mathrm{pu}} \approx E_g$. The linear development of the metallic weight is one of the features of photoconductivity due to photodoping based on the rigid band. On the other hand, the physical significance of the nonlinear development of the metallic weight could be profound. It is well known that, in a 1D Mott insulator, the strong enhancement of the nonlinear charge response results due to the large dipole moment from the almost degenerate odd and even excited states, especially near resonant optical excitation.[12,13] We note that, because of such a strong nonlinear response, $\mathcal{V}$ would no longer be a small perturbation for $\mathcal{H}_0$ in Eq. (1). This suggests that the electronic structure undergoes a nontrivial change in the form of phase transition at this resonant pumping.[14] The most direct way to confirm these two distinguishable processes of metallic switching would be ILPES.[15]

For ILPES, we extend our model Hamiltonian $\mathcal{H}$ to include photoemission terms and have

$$\mathcal{H} = \mathcal{H}_0 + \mathcal{V}(\tau) + \sum_{\mathbf{k}\sigma} \varepsilon_{\mathbf{k}} c^{\dagger}_{\mathbf{k}\sigma} c_{\mathbf{k}\sigma} + \mathcal{V}_{\mathrm{pes}}(\tau - \Delta),$$

$$\mathcal{V}_{\mathrm{pes}}(\tau) = A_{\mathrm{pes}} \sum_{\mathbf{k}l\sigma} c^{\dagger}_{\mathbf{k}\sigma} c_{l\sigma} e^{i\omega_{\mathrm{pes}}\tau} \Theta(\tau) + \mathrm{H.c.}, \tag{4}$$

where $c^{\dagger}_{\mathbf{k}\sigma}(c_{\mathbf{k}\sigma})$ is the photoelectron with its kinetic energy $\varepsilon_{\mathbf{k}}=\mathbf{k}^2/2$ and ω_{pes} and A_{pes} are the energy and the strength of the photon source adopted for the photoemission, respectively. MTD can also be applied to the calculation of ILPES. It is necessary to extend the Hilbert space to include all the relevant states spanned by $\Pi_l|\psi^j_l\rangle$ and $|\mathbf{k}\sigma\rangle\Pi_l|\psi^j_l\rangle$, where $|\mathbf{k}\sigma\rangle$ is the state of the photoelectron. Accordingly, the quantum state of the whole system should be $|\Psi(\tau)\rangle = \Sigma_{\{i\}} C_{\{i\}}(\tau)\Pi_l|\psi^j_l\rangle + \Sigma_{\mathbf{k}\sigma}\Sigma_{\{i\}} C^{\mathbf{k}\sigma}_{\{i\}}(\tau)|\mathbf{k}\sigma\rangle\Pi_l|\psi^j_l\rangle$ and ILPES can then be simply obtained as $\Sigma_\sigma \Sigma_{\{i\}} |C^{\mathbf{k}\sigma}_{\{i\}}(\tau)|^2$ from the solution of the time-dependent Schrödinger equation $i\partial/\partial\tau|\Psi(\tau)\rangle = \mathcal{H}|\Psi(\tau)\rangle$ in the limit of $A_{\mathrm{pes}} \to 0$ when $\tau > \Delta$. Solution of the finite size Hubbard model by exact diagonalization does not decay. Therefore, in the same way as the optical conductivity $\sigma(\omega)$, ILPES has no explicit time dependence when $\tau > \Delta$ except for the very short time range just after $\tau=\Delta$ (up to $\tau \sim 1.2\Delta$; the artificial effect of the step function cutoff of the pumping pulse could appear). In an actual experimental situation, on the other hand, the metallic phase is evanescent in $\mathcal{O}(1)$ picoseconds[4] and ILPES should be replaced by time-resolved photoemission spectroscopy (TRPES).[16]

ILPES and schematic sketches of the corresponding photoinduced electronic structures [i.e., density of states (DOS)] are provided in Fig. 4. The occupied (hatched) parts of those sketches can be directly compared with ILPES. For the photoinduced nonequilibrium state, as a matter of fact, the concept of "band structure" or "DOS" might not be clearly defined.[17] One possible way to avoid the difficulty is to define such concepts through the spectroscopy. That is, ILPES (generally, TRPES) itself is defined as the photoinduced band structure in this study. It is most interesting to find the finite DOS between the original upper and lower

Hubbard bands, i.e., in the gap region, in ILPES under the resonant pumping of Fig. 4(b). From such qualitative changes of ILPES compared to PES without optical pumping in Fig. 4(a), the nontrivial photoinduced band mixing is addressed. The driving force should be the nonperturbative effect of $\mathcal{V}$ due to the strongly enhanced nonlinearities. The change of electronic structures by the electric driving force could also be understood within the ac Stark effect which describes the shift of electronic energy levels under optical pumping.[18] On the other hand, no significant change of ILPES compared to PES under the off-resonant pumping addresses that the overall electronic structure is rigid. In Fig. 4(c), the induced density of states is accumulated only at the lower edge of the upper Hubbard band. To conclude, ILPES shows that there should be two qualitatively different dynamical processes for the metallic switching and confirms the conclusion from the study of the photoinduced optical conductivity.

In summary, we find the photoinduced Hubbard band mixing of the 1D half-filled Hubbard model from an analysis of the optical conductivity induced by ultrashort laser pumping, together with the direct investigation of the change of electronic structures through ILPES. The photoinduced weights evolve below the energy gap and they are attributed to the Drude weights in the thermodynamic limit. The nonlinear behavior of metallic weights at the resonant pumping directly demonstrates the reconstruction of electronic states as shown in ILPES, meaning the rigid band picture is not valid. This is in contrast to the case of the linear behavior at off-resonant pumping.

We acknowledge constructive discussions with Masao Arai, Kaoru Iwano, Takeshi Ogasawara, and Kenji Yonemitsu. This work was supported by Special Coordination Funds for Promoting Science and Technology from MEXT, Japan.

[1] M. Ashida, T. Ogasawara, Y. Tokura, S. Uchida, S. Mazumdar, and M. Kuwata-Gonokami, Appl. Phys. Lett. **78**, 2831 (2001).
[2] Y. Tokura, J. Phys. Soc. Jpn. **75**, 011001 (2006); K. Yonemitsu and K. Nasu, *ibid.* **75**, 011008 (2006), and references therein.
[3] M. Fiebig, K. Miyano, Y. Tomioka, and Y. Tokura, Science **280**, 1925 (1998); A. Cavalleri, Cs. Toth, C. W. Siders, J. A. Squier, F. Raksi, P. Forget, and J. C. Kieffer, Phys. Rev. Lett. **87**, 237401 (2001); M. Chollet, L. Guerin, N. Uchida, S. Fukaya, H. Shimoda, T. Ishioka, K. Matsuda, T. Hasegawa, A. Ota, H. Yamochi, G. Saito, R. Tazaki, S. Adachi, and S. Koshihara, Science **307**, 86 (2005).
[4] S. Iwai, M. Ono, A. Maeda, H. Matsuzaki, H. Kishida, H. Okamoto, and Y. Tokura, Phys. Rev. Lett. **91**, 057401 (2003); S. Iwai and H. Okamoto, J. Phys. Soc. Jpn. **75**, 011007 (2006).
[5] M. Imada, A. Fujimori, and Y. Tokura, Rev. Mod. Phys. **70**, 1039 (1998), and references therein.
[6] N. Maeshima and K. Yonemitsu, J. Phys. Soc. Jpn. **74**, 2671 (2005).
[7] J. D. Lee and M. Nishino, Phys. Rev. B **72**, 195111 (2005); J. D. Lee and J. Inoue, *ibid.* **73**, 165404 (2006); J. D. Lee, J. Inoue, and T. Kuroda, J. Phys. Soc. Jpn. **75**, 053703 (2006).
[8] J. D. Lee, J. Inoue, and M. Hase, Phys. Rev. Lett. **97**, 157405 (2006).
[9] G. D. Mahan, *Many-Particle Physics* (Plenum, New York, 1986).
[10] S. Moukouri, C. Huscroft, and M. Jarrell, in *Computer Simulations in Condensed Matter Physics VII*, edited by D. P. Landau, K. K. Mon, and H. B. Schuttler (Springer-Verlag, Berlin, 2000); finite size simulation with $N=8$ is found to capture the essential physics of the half-filled 1D Hubbard model through a systematic comparison with the results of the dynamical cluster approximation (DCA). DCA could overcome the finite size effect by keeping consistency between a cluster and the remaining bath in the same spirit as dynamical mean field theory. Although an application of DCA to the present time-dependent problem is not straightforward and beyond our scope, it suggests an important problem.
[11] W. Stephan and P. Horsch, Phys. Rev. B **42**, 8736 (1990); A. Moreo and E. Dagotto, *ibid.* **42**, 4786 (1990); E. Dagotto, Rev. Mod. Phys. **66**, 763 (1994), and references therein.
[12] Y. Mizuno, K. Tsutsui, T. Tohyama, and S. Maekawa, Phys. Rev. B **62**, R4769 (2000).
[13] M. Ono, K. Miura, A. Maeda, H. Matsuzaki, H. Kishida, Y. Taguchi, Y. Tokura, M. Yamashita, and H. Okamoto, Phys. Rev. B **70**, 085101 (2004); M. Ono, H. Kishida, and H. Okamoto, Phys. Rev. Lett. **95**, 087401 (2005).
[14] Our approach corresponds to the nonperturbative calculation of the S matrix, which properly gives the dynamical change of the underlying electronic structure at resonant pumping.
[15] J. Y. Son, T. Mizokawa, J. W. Quilty, K. Takubo, K. Ikeda, and N. Kojima, Phys. Rev. B **72**, 235105 (2005).
[16] L. Perfetti, P. A. Loukakos, M. Lisowski, U. Bovensiepen, H. Berger, S. Biermann, P. S. Cornaglia, A. Georges, and M. Wolf, Phys. Rev. Lett. **97**, 067402 (2006).
[17] By a quick consideration, one may try to replace the ground state by a photoinduced state for Green's function. However, it is not well defined such that its imaginary part tends to give unphysical negative spectral weights (Ref. 6).
[18] A. Mysyrowicz, D. Hulin, A. Antonetti, A. Migus, W. T. Masselink, and H. Morkoc, Phys. Rev. Lett. **56**, 2748 (1986); S. Schmitt-Rink and D. S. Chemla, *ibid.* **57**, 2752 (1986).